Journal of Inorganic Biochemistry 155 (2016) 76–81

Contents lists available at ScienceDirect

Journal of Inorganic Biochemistry

journal homepage: www.elsevier.com/locate/jinorgbio

Photochemical studies and nanomolar photodynamic activities of phthalocyanines functionalized with 1,4,7-trioxanonyl moieties at their non-peripheral positions

Lukasz Sobotta [a,1], Marcin Wierzchowski [b,1], Michal Mierzwicki [b], Zofia Gdaniec [c], Jadwiga Mielcarek [a], Leentje Persoons [d], Tomasz Goslinski [b], Jan Balzarini [d,*]

[a] Department of Inorganic and Analytical Chemistry, Poznan University of Medical Sciences, Grunwaldzka 6, 60-780 Poznan, Poland
[b] Department of Chemical Technology of Drugs, Poznan University of Medical Sciences, Grunwaldzka 6, 60-780 Poznan, Poland
[c] Institute of Bioorganic Chemistry, Polish Academy of Sciences, Z. Noskowskiego 12, 61-704 Poznan, Poland
[d] Rega Institute for Medical Research, KU Leuven, Minderbroedersstraat 10, B-3000 Leuven, Belgium

ARTICLE INFO

Article history:
Received 13 July 2015
Received in revised form 18 September 2015
Accepted 10 November 2015
Available online 14 November 2015

Keywords:
Antiviral photodynamic therapy
Cytostatic photodynamic therapy
Photosensitizer
Phthalocyanine
Singlet oxygen

ABSTRACT

Manganese(III), cobalt(II), copper(II), magnesium(II), zinc(II) and metal-free phthalocyanines, possessing 1,4,7-trioxanonyl substituents, at their non-peripheral positions, were subjected to photochemical, photodynamic and biological activity studies. Demetallated phthalocyanine and its metallated d-block analogues, with copper(II), cobalt(II), manganese(III) chloride, were found to be less efficient singlet oxygen generators in comparison to the zinc(II) analogue and zinc(II) phthalocyanine reference. Irradiation of several phthalocyanines for short time periods resulted in a substantially increased cytostatic activity against both suspension (leukemic/lymphoma at 85 nM) and solid (cervix carcinoma at 72 nM and melanoma at 81 nM) tumour cell lines (up to 200-fold). Noteworthy is that enveloped viruses, such as for herpesvirus and influenza A virus, but not, non-enveloped virus strains, such as Coxsackie B4 virus and reovirus-1, exposed to irradiation in the presence of the phthalocyanines, markedly lost their infectivity potential.

1. Introduction

Phthalocyanines (Pcs) are macrocyclic molecules consisting of four isoindole units linked by aza nitrogen atoms [1,2]. The aromatic character of Pcs impacts their spectral and electrochemical properties. Applications of Pcs have been increasing. Although, historically, they have been mainly used in the dye industry with copper phthalocyanine as the well-known pigment [3]. Nowadays, their applications are extended towards energy production (solar cells), electronics (laser printers, LCD displays, switches, recordable CDs) and medicine (photosensitizers) [4–8].

Pcs as photosensitizers have been applied on a regular basis in clinical and preclinical treatment for photodynamic diagnosis (PDD), photodynamic inactivation of bacteria and viruses (PACT), photodynamic treatment of skin disorders, and photodynamic treatment of cancer (PDT) [9]. In PDT, after the absorption of light, Pcs undergo excitation to their singlet excited state and then revert back to the ground state with the emission of fluorescence (PDD) or undergo intersystem cross-switching to a relatively long live triplet excited state. The transfer of energy from the photosensitizer to molecular oxygen, which exists in its ground triplet state, is accompanied by the conversion to its excited singlet state and production of singlet oxygen. Singlet oxygen is a common reactive oxygen agent able to kill cancer cells and microorganisms [10]. PDT seems to possess potential in the treatment of skin melanoma with the destruction of melanoma cells and only minimal side-effects to skin fibroblasts. The therein applied PDT was found to generate photocytotoxicity against cancer and enhanced the immunological response [11,12].

A successful PDT treatment depends on a proper dosimetry, which is strictly connected with the use of light — defined wavelengths and their intensity, and a fixed dose of photosensitizer [13]. There is a constant interest in novel Pc photosensitizers for photodynamic therapy. The main drawback is that the currently available Pcs in medicine have poor solubility in water, which limits their administration in vitro or in vivo. Therefore, there is a continuing interest in novel Pcs with good solubility in water and high singlet oxygen generation. One option in obtaining useful photosensitizers for PDT is to develop a proper drug delivery system [14,15]. Another possibility is to use peripheral substituents increasing the Pcs solubility (e.g. sulphonic, carboxylic, pyridyloxy groups) [16–18]. Lately, we reported the synthesis, characterization, as well as photodynamic biological properties of the series of Pc analogues,

* Corresponding author.
E-mail address: jan.balzarini@rega.kuleuven.be (J. Balzarini).
[1] These authors contributed equally to the work presented here and should therefore be regarded as equivalent authors.

http://dx.doi.org/10.1016/j.jinorgbio.2015.11.006
0162-0134/

equipped with polyetheroxy substituents at their non-peripheral positions [19].

In our research, we focused on the photochemical, photodynamic and the biological properties of novel polyetheroxy-substituted Pc analogues. The demetallated phthalocyanine and its complexes with various metal ions in the centre, were subjected to biological tests on cancer cell lines and selected viruses.

2. Results and discussion

2.1. Chemistry

The novel metal-free phthalocyanine **4** was obtained with 33% yield by adapting the demetallation reaction conditions previously described [20,21]. The standard reaction time of **3** with TFA was extended from 0.5 to 3 h. Interestingly, a decreased reactivity of compound **3** was probably due to the presence of polyether peripheral chains impeding the access of protonic acid to the macrocyclic core. Subsequent remetallation was based on the reaction of **4** with metal chlorides in DMF at a temperature of 70 °C for 24 h and led to the products **5a**–**5c** with differentiated yields (Scheme 1) [22]. Noteworthy, in the remetallation reaction, various salt species revealed differentiated reactivity and can be ordered in terms of their decreasing efficiency in the following way: $MnCl_2 \cdot 4H_2O$ (yield 69%), $CoCl_2 \cdot 4H_2O$ (yield 53%) and $CuCl_2$ (yield 15%). All new macrocyclic compounds were purified on silica gel by flash column chromatography in normal and reversed-phase system and on cross-linked dextran gel (Sephadex) by size-exclusion chromatography. HPLC analyses confirmed the purity of the macrocyclic compounds **4**, **5a**–**5c** at a level above 95%. New metal-free phthalocyanine **4** was characterized using ^1H and ^{13}C NMR spectroscopy. In the ^1H NMR spectrum of the symmetrical phthalocyanine **4**, only one singlet at 8.02 ppm, corresponding to the aromatic protons, was observed. In the aliphatic region five resonances of methylene groups and one of the methyl groups of the polyetheroxy chains were identified: triplets at 5.35, 4.38, 3.93, 3.65, 1.08 ppm and a quartet at 3.41 ppm, respectively. Protons of the adjacent methylene groups and the methyl groups of the polyethylene chains were assigned using ^1H–^1H COSY spectrum (Fig. 1). Singlet at 0.07 ppm was attributed to core pyrrole-H protons.

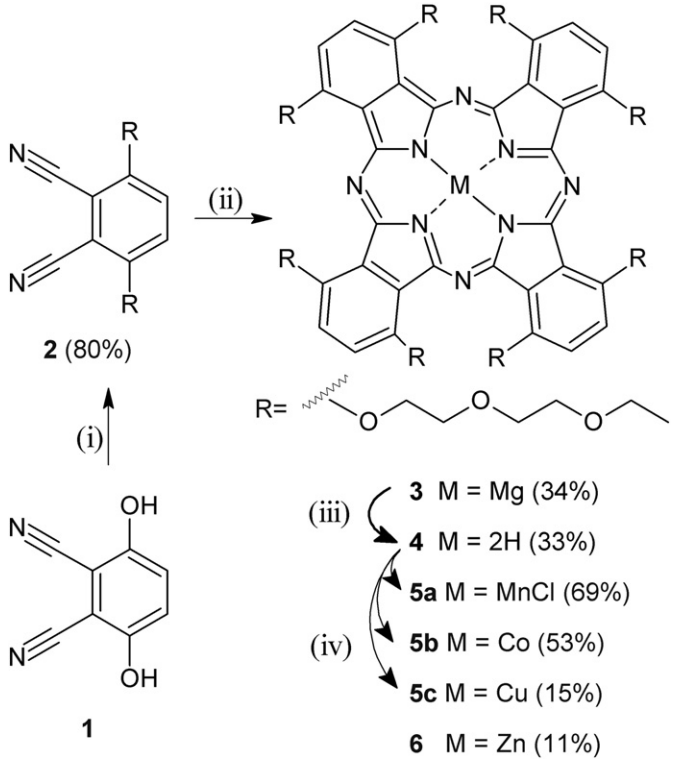

Scheme 1. Reagents and conditions: (i) $Br(CH_2CH_2O)_2CH_2CH_3$, K_2CO_3, DMF, 70 °C, 24 h (80%); (ii) **3** — $Mg(OnBu)2$, *n*BuOH, reflux, 20 h (33%), **6** — *n*PeOH, $Zn(OAc)_2$, reflux, 24 h (11%); (iii) TFA, CH_2Cl_2, r.t., 3 h (34%); (iv) given metal salt, DMF, 70 °C, 24 h.

Carbon resonances within a ^{13}C NMR spectrum of Pc **4** were unambiguously assigned, using a combination of two-dimensional techniques such as HSQC (Heteronuclear Single Quantum Coherence) and HMBC (Heteronuclear Multiple Bond Correlation). ^1H and ^{13}C chemical shifts of Pc **4**, together with key HMBC and ^1H–^1H COSY, correlations are shown in Fig. 1.

2.2. Photostability

Photosensitizers can undergo two types of photochemical reactions — phototransformation and photobleaching, eventually both of them. The nature of the decomposition process depends on many factors including the chemical structure of the investigated compound, the solvent used and the concentration of the molecular oxygen. The progress of phototransformation may be studied in the UV–vis through the appearance of new absorption bands. Opposite to this, in the photobleaching process, a disappearance of absorption bands in the visible region can be observed resulting in the loss of the dye colour [23]. Photobleaching of **6** is shown in Fig. 2. According to the literature, the main photoproduct, which is characteristic for phthalocyanine decomposition in the presence of molecular oxygen is phthalimide. The phthalimide formation, which stems from phthalocyanine, is a typical Diels-Alder cycloaddition of singlet oxygen, which is generated by phthalocyanine in the photodynamic reaction [23,24].

Studied Pcs underwent photobleaching in DMF and DMSO. There was no evidence of any new bands in their absorption spectra during irradiation, whereas a disappearance of Pc Soret and Q-band was observed. Some compounds (Table 1S, Supplementary data) decomposed in two stages, according to the first order kinetic reaction. The first step taken in photobleaching may be due to the formation of the cycloadduct of Pc indole fragment with an excited form of molecular oxygen. The second one is the result of the adduct decomposition to phthalimide. Interestingly, some of the investigated compounds showed photodegradation in one stage, possibly due to the very fast first step of decomposition.

The quantum yields of photobleaching were determined according to a method presented by Seotsanyana-Mokhosi et al. [25]. Quantum yields of photobleaching observed in the compounds dissolved in DMSO were much lower than that of the DMF (Table 2S, Supplementary data), and can be explained through the coordination-interaction between the macrocycle core metal ion and DMSO [26,27]. A confirmation of the stabilizing effect of DMSO in the photobleaching process is the result obtained for **4** in comparison to that measured for the other metallated analogues **3**, **5a**–**5c** and **6**. It was found that the quantum yields of photobleaching in DMF and DMSO differ less in the case of **4** as compared to the other macrocycles studied. It is probably due to the absence of metal ions in the core of Pc **4**. In addition, a little lower quantum yield in DMSO of **4** was probably the result of the DMSO viscosity or the dielectric constant. Photobleaching was performed both in aerobic conditions and with limited access to air (nitrogen bubbling in solution for 20 min). Measurements performed for **3**, **4**, **5a** and **5c** showed a decrease in the photobleaching quantum yields under conditions limiting access to air, in comparison to the results achieved under aerobic conditions (Table 2S, Supplementary data). This is a result of the limited access to molecular oxygen, more specifically to a lower singlet oxygen formation. A particular phenomenon was observed for **6**, which is the most effective singlet oxygen generator. Moreover, similar quantum yields of photobleaching both in aerobic conditions and at limited access to air were found for **6**. Interestingly enough, **5b** in DMF decomposed much faster under limited access to air than in aerobic conditions. This phenomenon commits radical photoreactions with DMF. Furthermore, in DMSO solution Pc **5b** revealed similar quantum yields under both conditions used, (i) a limited access to air and (ii) aerobic

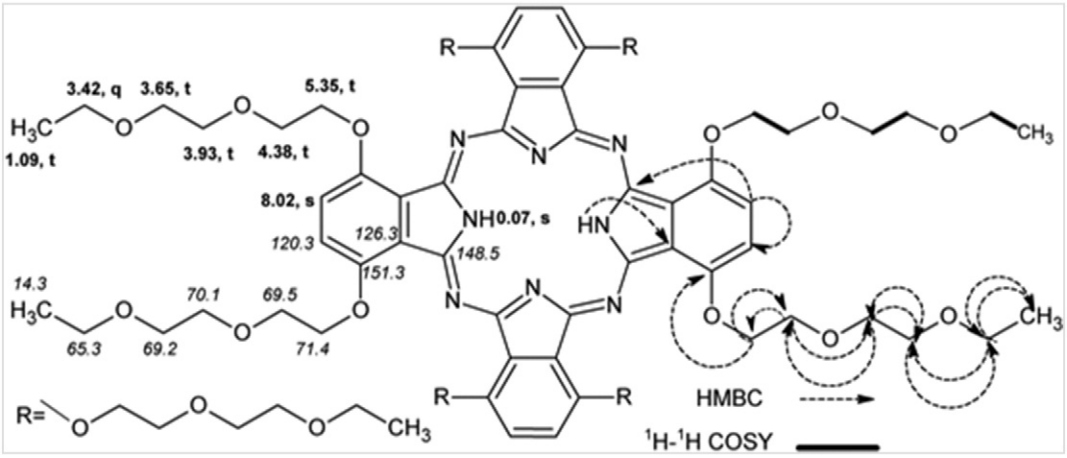

Fig. 1. ^{1}H and ^{13}C chemical shifts [ppm] of **4** in pyridine-d_5. Key HMBC and ^{1}H–^{1}H COSY correlations are marked with dashed arrows and bold lines, respectively.

conditions. The lowest quantum yields within the photodecomposition process for all compounds studied, under aerobic conditions, were found for **5b** in DMF and **5a** in DMSO. The highest values of quantum yield decomposition were found for **3** in DMF solution and **4** in DMSO solution.

2.3. Singlet oxygen

One of the most important properties of phthalocyanines is their ability to generate various reactive oxygen species, including singlet oxygen. Singlet oxygen possesses a high oxidizing potential and therefore, has been utilized in different areas of life such as: cancer treatment using photodynamic therapy, photooxidation of toxic molecules in the waste water treatment, and in chemical synthesis [28,29].

Within all the investigated Pcs, compound **6** was found to be the most efficient singlet oxygen generator [19] (Table 1). Demetallated Pc and its metallated d-block analogues, with copper(II), cobalt(II), manganese(III) chloride, were found to be less efficient. This fact can be explained through the metal ion influence on the electronic energy levels of the molecule. Open shell coordinated metal ions, such as Mn^{3+}, Cu^{2+}, or Co^{2+}, influence the short living excited state of macrocycle, as compared to closed shell metal ions, such as Mg^{2+} or Zn^{2+}. This phenomenon directly influences the singlet oxygen generation efficacy. Within closed shell metal ions incorporated to the core of macrocycles, zinc is known to cause the highest values of singlet oxygen generation. It is the result of the well-known "heavy atom effect", which is connected with the spin–orbit coupling phenomenon [26–28]. Additionally, further studies performed under conditions with limited access to air resulted in a decrease of singlet oxygen generation ability, indicating its dependency on the oxygen presence (Table 3S, Supplementary data).

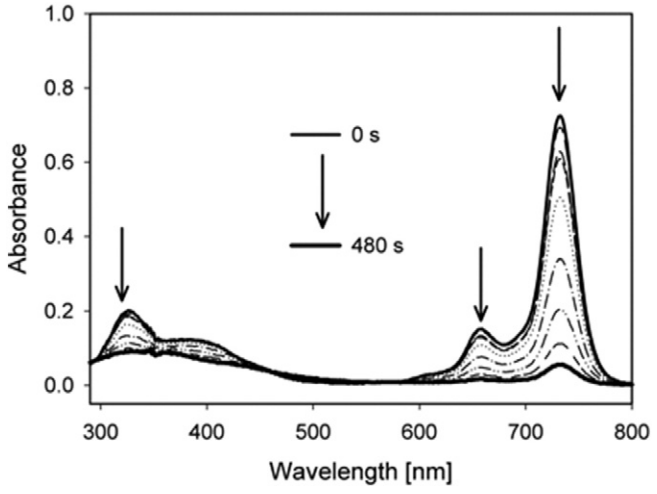

Fig. 2. Changes in the absorption spectra of phthalocyanine **6** in DMF solution after exposure to radiation.

2.4. Biological studies

In a first series of experiments, the cytostatic activity of a variety of phthalocyanine derivatives was studied in three different human tumour cell models including CD_4^+ T-lymphoblast CEM cells growing in suspension, and the solid tumour-derived cervix carcinoma HeLa and melanoma SK-MEL-5 cells growing in monolayers. When administered to tumour cell cultures for 3 to 4 days of incubation time at 37 °C, a moderate cytostatic activity in the test compounds was observed. A 50% inhibitory concentration (IC_{50}) against tumour cell proliferation was within the same order of magnitude for each compound. Compounds **3**, **5b**, **5c** and **6** that contain, respectively, Mg^{2+}, Co^{2+}, Cu^{2+} or Zn^{2+} in their core were the most cytostatic compounds (IC_{50}: 4.8–7.7 μM for CEM, 6.8–19 μM for HeLa and 5.7–6.6 μM for SK-MEL-5). Metal-free **4** and phthalocyanine **5a** containing Mn^{3+} in their core showed poor, if any cytostatic activity (IC_{50}: 20–>50 μM for the three tumour cell lines) (Table 2).

The tumour cell cultures were irradiated at 735 nm for 30 min at the start of the tumour cell incubation (day 0): day 1 (after 24 h) and, day 2

Table 1
Quantum yields of singlet oxygen generation of phthalocyanines **3**–**6** and reference compound (**ZnPc**) [30,31].

Pcs	Solvent	Irradiation wavelength λ [nm]	Quantum yields of singlet oxygen generation $\Delta\Phi \pm \Delta\Phi$	
			Aerobic conditions	Limited access to air
3 [19]	DMF	732	0.32 ± 0.01	0.27 ± 0.01
	DMSO	739	0.30 ± 0.01	0.22 ± 0.01
4	DMF	757	<0.01	<0.01
	DMSO	764	<0.01	<0.01
5a	DMF		Insoluble	
	DMSO	826	<0.01	<0.01
5b	DMF	718	0.02 ± <0.01	<0.01
	DMSO	723	0.02 ± <0.01	<0.01
5c	DMF	736	0.02 ± <0.01	<0.01
	DMSO	740	<0.01	<0.01
6 [19]	DMF	731	0.46 ± 0.02	0.35 ± 0.02
	DMSO	740	0.47 ± 0.02	0.40 ± 0.02
ZnPc [30,31]	DMF	670	0.56	
	DMSO	672	0.67	

Table 2
Effect of tumour cell culture irradiation at λ = 735 nm.

Compound	IC_{50}[a] (μM)					
	CEM		HeLa		SK-MEL-5	
	Dark	Irradiation at 735 nm	Dark	Irradiation at 735 nm	Dark	Irradiation at 735 nm
3	7.7 ± 0.2	1.5 ± 0.2	14 ± 6	0.85 ± 0.41	–	–
4	20 ± 7	0.085 ± 0.011	>50	0.32 ± 0.29	≥50	0.34 ± 0.28
5a	20 ± 4	19 ± 8	>50	>50	–	–
5b	7.1 ± 1.5	3.2 ± 0.9	13 ± 3	4.9 ± 0.4	–	–
5c	4.8 ± 0.1	0.13 ± 0.03	19 ± 11	0.38 ± 0.29	6.6 ± 2.3	0.33 ± 0.15
6	5.4 ± 1.1	0.50 ± 0.46	6.8 ± 6.0	0.072 ± 0.032	5.7 ± 2.3	0.081 ± 0.052

[a] 50% Inhibitory concentration or compound concentration required to inhibit tumour cell proliferation by 50%.

(after 48 h). Tumour cell growth was determined on day 3 (CEM) or day 4 (HeLa, SK-MEL-5).

In a second series of experiments, the tumour cell cultures to which the compounds were administered, were irradiated for 30 min at 735 nm with a light intensity of 4.5 mW/cm^2 (total light dose for each irradiation 8.1 J/cm^2) at the beginning of the cell-drug cultivation (day 0), at day 1 and at day 2 of the experiment. Under these experimental conditions, several compounds became exquisitely toxic to the tumour cells. It should be noticed that the irradiation sequence used (3 subsequent days for 30 min) did not affect the tumour cell growth in the absence of the compounds. The degree of increased cytostatic potential upon irradiation of the compound-exposed tumour cell cultures highly differed depending the nature of the compounds. For example, whereas the irradiation of compound **5a** had no effect on its (poor) cytostatic activity, and only a slight effect (2- to 3-fold increased cytostatic activity) on compound **5b** was observed, a dramatic increase of cytostatic activity was found for compounds **3**, **4**, **5c** and **6** (Table 2). Depending the nature of the tumour cell lines and the compound, cytostatic activity was increased by 5- to 200-fold for CEM, 20- to 100-fold for HeLa, and 20- to 100-fold for SK-MEL-5 cells. The most striking activities were found for compound **4** where irradiation at λ 735 nm caused a 100- to 200-fold increased antiproliferative activity irrespective of the tumour cell line evaluated (Table 2).

Control values are set as 100% infectivity upon titration and CCID50 determination.

In a third set of experiments, compound **5c** (100 μM) was exposed to several virus strains, irradiated for 30 min at 735 nm and after irradiation the compound/virus was added to confluent human embryonic lung (HEL), African green monkey kidney (Vero) or Madin-Darby canine kidney (MDCK) cell cultures. Whereas, the irradiation treatment had no effect on the virus-induced cytopathicity for Coxsackie virus B4 and reovirus-1; there was a dramatic drop of the virus infectivity in the cell cultures infected with herpes simplex virus type 1 (30- to 350-fold), parainfluenza virus-3 (20- to 25-fold), Punta Toro virus (>25- to 200-fold), Sindbis virus (>70 to >125-fold), and influenza virus A (H1N1, H3N2) (>25- to 180-fold) and B (2.5- to 7-fold) (2 independent experiments in duplicate) (Table 3). Thus, short irradiation of phtalocyanine derivatives can substantially decrease in the infectivity of enveloped viruses, such as for herpesvirus and influenza A virus, but not for non-enveloped viruses such as Coxsackie B4 virus and reovirus-1.

3. Conclusions

The findings here indicate that phthalocyanine derivatives are light-dependent inhibitors of tumour cell proliferation and decrease the infectivity of a wide variety of enveloped viruses. This opens-up an interesting area in the development of a novel type of chemotherapeutic class of agents. They may provide a selective basis for the treatment of local (i.e. dermatological) diseases through the activation of medications through a light-exposed biological (i.e. skin) surface, with minimal effects on the whole host organism. This approach is fundamentally different from other photochemotherapeutic approaches that target DNA through direct drug interaction, as is the case for 8-methoxypsoralen and proflavine, after being exposed to long-wave ultraviolet irradiation [32,33]. The phthalocyanine irradiation, with wavelengths in the far-red light spectrum, is much less damaging for near-by tissues of the object being irradiated, and affords its activity by the local generation of various reactive oxygen species, including singlet oxygen.

4. Experimental

4.1. Materials and methods

All reactions were conducted in oven-dried glassware under nitrogen. Reported reaction temperatures refer to the external bath temperatures. All reactions were performed under an inert atmosphere of nitrogen. All solvents were evaporated under reduced pressure using a rotavap, below 60 °C. All solvents and reagents were obtained from commercial suppliers and used without further purification. Melting points

Table 3
Infectivity potential of viruses after irradiation for 30 min at λ = 735 nm in the presence of **5c**.

Virus strain	Infectivity upon 30′ irradiation in the presence of compound 5c (percent of control)[a]		Average percentage of virus infectivity versus control
	Experiment 1	Experiment 2	
Herpes simplex virus type 1 (KOS)	3	0.27	1.6
Parainfluenza virus-3	3.9	5.2	4.6
Punta Toro virus	<0.46	<4	<2.2
Sindbis virus	<0.80	<1.4	<1.1
Influenza A virus			
H1N1	<2.7	0.55	<1.6
H3N2	<2.7	4	<3.3
Influenza B virus	45	15	30
Coxsackie virus B4	110	85	98
Reovirus-1	100	76	88

were obtained on a "Stuart" Bibby apparatus and were not corrected. Dry flash column chromatography was carried out on Merck silica gel 60, particle size 40–63 μm and Fluka silica gel 90 C18 — reversed phase. Size-exclusion chromatography was performed on Sephadex G-25. Thin layer chromatography (TLC) was performed on silica gel Merck Kieselgel 60 F 254 plates and DC Kieselgel 60 RP-18 F254 and visualized with UV illumination (λ_{max} 254 or 365 nm). Mass spectrometry experiments (ES, MALDI TOF) and elemental analyses were carried out at the Advanced Chemical Equipment and Instrumentation Facility at the Faculty of Chemistry, Adam Mickiewicz University in Poznan. The UV–visible (UV–vis) spectra were recorded on Hitachi UV/VIS U-1900 and Shimadzu UV-160A spectrometers; λ_{max} [nm] (log ε). 1D and 2D NMR experiments were carried out using a Bruker 400 spectrometer. Chemical shifts (δ) are quoted in parts per million (ppm) and refer to a residual solvent peak. Coupling constants (J) are quoted in Hertz (Hz) to the nearest 0.5 Hz. The abbreviations s, t, h and q refer to singlet, triplet, hidden and quartet, respectively. ^{1}H and ^{13}C signals were assigned using ^{1}H–^{1}H COSY, HSQC and HMBC experiments. Analytical HPLC was performed on an Agilent 1200 Series instrument.

4.2. Synthesis

Known compounds, 2,3-dicyanohydroquinone **1**, 3,6-bis(1,4,7-trioxanonyl)-1,2-benzenedicarbonitrile **2**, [1,4,8,11,15,18,22,25-octakis(1,4,7-trioxanonyl)phthalocyanine]magnesium(II) **3**, and [1,4,8,11,15,18,22,25-octakis(1,4,7-trioxanonyl)phthalocyanine]zinc(II) **6** were synthesized following previously published procedures [19].

4.2.1. 1,4,8,11,15,18,22,25-octakis(1,4,7-trioxanonyl)phthalocyanine (*4*)

Suspension of [1,4,8,11,15,18,22,25-octakis(1,4,7-trioxanonyl) phthalocyanine]magnesium(II) (**3**) (100 mg, 0.06 mmol) was rapidly mixed in trifluoroacetic acid (25 mL) for 3 h. Next, reaction contents were poured into water and ice mixture (200 mL) and neutralized with concentrated solution of sodium bicarbonate. Resulting solution was extracted with CH_2Cl_2 (200 mL) and combined organic layers were after drying with anhydrous $MgSO_4$ were evaporated to dryness. Column chromatography (CH_2Cl_2:CH_3OH 15:1) was performed to give dark green solid **4** (34 mg, 33% yield). M.p. > 50 °C (mesophase behaviour). R_f (THF:CH_3OH 15:1) 0.65. UV–vis (CH_2Cl_2): λ_{max} [nm] (log ε): 757 (5.10), 670 (4.54), 396 (4.32), 333 (4.69). MS (MALDI-TOF): *m/z* $[M + H]^+$ 1572.7. ^{1}H NMR (400 MHz, pyridine-d_5) δ: 8.02 (s, 8 H), 5.35 (t, ^3J = 4.5 Hz, 16 H), 4.38 (t, ^3J = 4.5 Hz, 16 H), 3.93 (t, ^3J = 5.0 Hz, 16 H), 3.65 (t, ^3J = 5.0 Hz, 16 H), 3.41 (q, ^3J = 7.0 Hz, 16 H), 1.08 (t, ^3J = 7.0 Hz, 24 H), 0.07 (s, 2 H). ^{13}C NMR (101 MHz, pyridine-d_5) δ: 151.3, 148.5^h (present only as a cross-peak in HMBC), 126.3, 120.1, 71.4, 70.1, 69.5, 69.2, 65.3, 14.3. HPLC (Supplementary data) purity 95.10–96.49%.

4.2.2. [1,4,8,11,15,18,22,25-octakis(1,4,7-trioxanonyl)phthalocyanine] manganese(III) chloride (*5a*)

A rapidly stirred mixture of phthalocyanine **4** (95 mg 0.06 mmol) and $MnCl_2 \cdot 4H_2O$ (57 mg 0.06 mmol) in 20 mL of DMF were heated at 70 °C for 24 h. After being allowed to cool to room temperature, the reaction mixture was filtered and evaporated to dryness under reduced pressure with toluene (60 mL). Dry residue was dissolved in CH_2Cl_2 (30 mL) and rapidly mixed with 30 mL of concentrated solution of sodium chloride for 30 min. Next, organic layer was separated, washed with water (60 mL) and dried with anhydrous $MgSO_4$. Organic solvent was evaporated under reduced pressure and dry residue was subjected to column chromatography (CH_2Cl_2:CH_3OH 15:1, EtOAc, CH_2Cl_2:CH_3OH 15:1) to give dark brown solid **5a** (66 mg, 69% yield). M.p. > 80 °C (mesophase behaviour). R_f (CH_2Cl_2:CH_3OH 15:1) 0.08. UV–vis (CH_2Cl_2) λ_{max} [nm] (log ε) 811 (4.96), 729 (4.34), 556 (4.18), 345 (4.53). MS (MALDI-TOF) [m/z] M^+ 1658.09, $[M\text{-}Cl]^+$ 1624.32. IR ν [cm^{-1}] 1070, 1213, 1309, 1503, 2866; HPLC (Supplementary data) purity 98.56–99.93%.

4.2.3. [1,4,8,11,15,18,22,25-octakis(1,4,7-trioxanonyl)phthalocyanine] cobalt(II) (*5b*)

A rapidly stirred mixture of phthalocyanine **4** (105 mg 0.07 mmol) and $CoCl_2 \cdot 6H_2O$ (79 mg 0.33 mmol) in 20 mL of DMF were heated at 70 °C for 24 h. After being allowed to cool to room temperature, the reaction mixture was filtered and evaporated to dryness under reduced pressure with toluene (60 mL). Column chromatography (CH_2Cl_2: CH_3OH 15:1, EtOAc, CH_2Cl_2:CH_3OH 4:1) and size-exclusion chromatography (Sephadex G-25, methanol) were performed to give dark brown solid **5b** (56 mg, 53% yield). M.p. > 40 °C (mesophase behaviour). R_f (CH_2Cl_2: MeOH 15:1) 0.18. UV–vis (CH_2Cl_2) λ_{max} [nm] (log ε) 727 (4.86), 655 (4.30), 374 (4.33), 321 (4.57). MS (MALDI-TOF) [m/z] $[M + H]^+$ 1629.3. IR ν [cm^{-1}] 1115, 1214, 1268, 1499, 1601, 2869. HPLC (Supplementary data) purity 95.81–100.00%.

4.2.4. [1,4,8,11,15,18,22,25-octakis(1,4,7-trioxanonyl)phthalocyanine] cooper(II) (*5c*)

A rapidly stirred mixture of phthalocyanine **4** (128 mg 0.08 mmol) and $CuCl_2$ (57 mg 0.06 mmol) in DMF (20 mL) were heated at 70 °C for 24 h. After being allowed to cool to room temperature, the reaction mixture was filtered and evaporated to dryness under reduced pressure with toluene (60 mL). Column chromatography (CH_2Cl_2:CH_3OH 20:1, EtOAc, CH_2Cl_2:CH_3OH 15:1) was performed to give dark green solid **5c** (19 mg, 15% yield). M.p. > 50 °C. R_f (CH_2Cl_2: CH_3OH 15:1) 0.16. UV–vis (CH_2Cl_2) λ_{max} [nm] (log ε) 740 (5.17), 662 (4.57), 438 (4.07) 326 (4.75). MS (MALDI-TOF) [m/z] $[M + H]^+$ 1633.3. IR ν [cm^{-1}] 1114, 1267, 1501, 1601, 2867; HPLC (Supplementary data) purity 98.38–100.00%.

4.3. Photostability

The photostability of the investigated compounds was tested both under aerobic conditions and with limited access to air. A high pressure xenon lamp and filter cutting-off wavelengths below 450 nm were applied. Experiments have been performed according to the method previously described [34].

4.4. Singlet oxygen generation

The quantum yield of singlet oxygen generation of Pcs was assessed using 1,3-diphenylisobenzofuran (DPBF, *Aldrich*). DPBF as a chemical quencher of singlet oxygen. Pc and DPBF solution was irradiated at a wavelength corresponding to the Q band of the tested macrocycle. The experimental procedure has been previously described in details [18,19,24,25,31,34].

4.5. Anti-proliferative assays

The cytostatic activity of the tested compounds on human CD4+ T-lymphocyte (CEM), human cervix carcinoma (HeLa) and human melanoma SK-MEL-5 cells was evaluated as follows: an appropriate number of tumour cells were suspended in RPMI-1640 growth medium and were seeded in 200 μl-wells of 96-well microtiter plates, in the presence (or absence for purposes of control) of variable concentrations of the test compounds. The cell cultures were irradiated with red light at 735 nm for 30 min with a light intensity of 4.5 mW/cm^2 (light dose 8.1 J/cm^2) (or not irradiated (control)) before incubation at 37 °C in a humidified CO_2-controlled atmosphere (day 0). Recorded on day 1 and day 2, the irradiated tumour cell cultures were exposed again to red light irradiation at 735 nm for 30 min, after which the cultures continued to be incubated at 37 °C. On day 3 (CEM) or day 4 (HeLa, SK-MEL-5), the number of cells were counted on a Coulter counter. The IC_{50} value was defined as the compound concentration required to inhibit tumour cell proliferation by 50%.

4.6. Antiviral activity assays

The effect of the exposure to (irradiated or non-irradiated) test compounds was evaluated for the following viruses: herpes simplex virus type 1 (HSV-1, strain KOS), Coxsackie virus B4, parainfluenza virus-3, Punta Toro virus, Sindbis virus, reovirus-1, influenza A virus (strains H1N1; H3N2) and influenza B virus. The infectivity was determined by titration of the virus stocks before and after irradiation for 30 min at 735 nm with a light intensity of 4.5 mW/cm^2 (light dose 8.1 J/cm^2) on MDCK (for influenza viruses) or Vero (for all other viruses) cell cultures. The initial irradiated virus stock solutions ($CCID_{50}$) were as follows: 10,663 (HSV-1), 85,506 (parainfluenza virus 3), 601 (Punta Toro virus), 50,389 (reovirus-1), 471 (Sindbis virus), 916 (influenza A, H1N1), 770 (influenza A, H3N2) and 496 (influenza B). Cell cultures (Vero, MDCK) were grown in 96-well microtiter plates to confluency (MDCK to 80% confluency) after which, a dilution series of irradiated versus non-irradiated virus was administered. Three days after the incubation of the cell cultures with the viral dilutions, the virus titers were determined as 50% cell culture infective doses ($CCID_{50}$), or the virus dose required to inhibit 50% of the number of infected cell cultures.

Acknowledgements

The authors thank Lizette van Berckelaer and Beata Kwiatkowska for excellent technical assistance. This study was supported by the National Science Centre under Grant No. N N401 067238. ZG thanks the European Fund for Regional Development for Grant No UDA-POIG.02.01.00-30-182/09. LS is a scholarship holder within the project "Scholarship support for Ph.D. students specializing in majors strategic for Wielkopolska's development", Sub-measure 8.2.2 Human Capital Operational Programme, co-financed by EU under the European Social Fund. LS acknowledges the Polish National Science Centre for granting him with a scholarship within the project "Etiuda 1" no. 2013/08/T/NZ7/00242. The biological experiments were performed with support of the KU Leuven (GOA 15/19 TBA).

Appendix A. Supplementary data

Supplementary data to this article can be found online at http://dx.doi.org/10.1016/j.jinorgbio.2015.11.006.

References

[1] A. Wang, L. Long, C. Zhang, Synthesis of unsymmetrical phthalocyanines: a brief overview, Tetrahedron 68 (2012) 2433–2451.
[2] J. Mack, N. Kobayashi, Low symmetry phthalocyanines and their analogues, Chem. Rev. 111 (2011) 281–321.
[3] C.G. Claessens, W.J. Blau, M. Cook, M. Hanack, R.J.M. Nolte, T. Torres, D. Wöhrle, Phthalocyanines and phthalocyanine analogues: the quest for applicable optical properties, Monatsh. Chem. 132 (2001) 3–11.
[4] D. Wöhrle, G. Schnurpfeil, S.G. Makarov, A. Kazarin, O.N. Suvorova, Practical applications of phthalocyanines — from dyes and pigments to materials for optical, electronic and photo-electronic devices, Macroheterocycles 5 (2012) 191–202.
[5] C.-B. Yao, Y. Zhang, D.-T. Chen, H.-T. Yin, C.-Q. Yu, J. Li, P. Yuan, Study of all-optical switching and optical limiting properties in phenoxy-phthalocyanines liquid, Opt. Laser Technol. 47 (2013) 228–231.
[6] W. Lee, S.B. Yuk, J. Choi, D.H. Jung, S.-H. Choi, J. Park, J.P. Kim, Synthesis and characterization of solubility enhanced metal-free phthalocyanines for liquid crystal display black matrix of low dielectric constant, Dyes Pigments 92 (2012) 942–948.
[7] M.-E. Ragoussi, M. Ince, T. Torres, Recent advances in phthalocyanine-based sensitizers for dye-sensitized solar cells: phthalocyanine-based sensitizers for dye-sensitized solar cells, Eur. J. Org. Chem. 2013 (2013) 6475–6489.
[8] L. Ryskova, V. Buchta, M. Karaskova, J. Rakusan, J. Cerny, R. Slezak, In vitro antimicrobial activity of light-activated phthalocyanines, Cent. Eur. J. Biol. 8 (2013) 168–177.
[9] R.R. Allison, C.H. Sibata, Oncologic photodynamic therapy photosensitizers: a clinical review, Photodiagn. Photodyn. Ther. 7 (2010) 61–75.
[10] A.P. Castano, T.N. Demidova, M.R. Hamblin, Mechanisms in photodynamic therapy: part one—photosensitizers, photochemistry and cellular localization, Photodiagn. Photodyn. Ther. 1 (2004) 279–293.
[11] P. Nowak-Sliwinska, A. Karocki, M. Elas, A. Pawlak, G. Stochel, K. Urbanska, Verteporfin, photofrin II, and merocyanine 540 as PDT photosensitizers against melanoma cells, Biochem. Biophys. Res. Commun. 349 (2006) 549–555.
[12] A. Kawczyk-Krupka, A.M. Bugaj, W. Latos, K. Zaremba, A. Sieroń, Photodynamic therapy in treatment of cutaneous and choroidal melanoma, Photodiagn. Photodyn. Ther. 10 (2013) 503–509.
[13] R.R. Allison, G.H. Downie, R. Cuenca, X.-H. Hu, C.J. Childs, C.H. Sibata, Photosensitizers in clinical PDT, Photodiagn. Photodyn. Ther. 1 (2004) 27–42.
[14] P. Skupin-Mrugalska, J. Piskorz, T. Goslinski, J. Mielcarek, K. Konopka, N. Düzgüneş, Current status of liposomal porphyrinoid photosensitizers, Drug Discov. Today 18 (2013) 776–784.
[15] A. Derycke, Liposomes for photodynamic therapy, Adv. Drug Deliv. Rev. 56 (2004) 17–30.
[16] V. Mantareva, V. Kussovski, I. Angelov, E. Borisova, L. Avramov, G. Schnurpfeil, D. Wöhrle, Photodynamic activity of water-soluble phthalocyanine zinc(II) complexes against pathogenic microorganisms, Bioorg. Med. Chem. 15 (2007) 4829–4835.
[17] N. Masilela, T. Nyokong, The synthesis and photophysical properties of water soluble tetrasulfonated, octacarboxylated and quaternised 2,(3)-tetra-(2 pyridiloxy) Ga phthalocyanines, Dyes Pigments 84 (2010) 242–248.
[18] M. Durmuş, A. Erdoğmuş, A. Ogunsipe, T. Nyokong, The synthesis and photophysicochemical behaviour of novel water-soluble cationic indium(III) phthalocyanine, Dyes Pigments 82 (2009) 244–250.
[19] M. Wierzchowski, L. Sobotta, P. Skupin-Mrugalska, J. Kruk, W. Jusiak, M. Yee, K. Konopka, N. Düzgüneş, E. Tykarska, M. Gdaniec, J. Mielcarek, T. Goslinski, Phthalocyanines functionalized with 2-methyl-5-nitro-1 H-imidazolylethoxy and 1,4,7-trioxanonyl moieties and the effect of metronidazole substitution on photocytotoxicity, J. Inorg. Biochem. 127 (2013) 62–72.
[20] T.P. Forsyth, D.B.G. Williams, A.G. Montalban, C.L. Stern, A.G.M. Barrett, B.M. Hoffman, A facile and regioselective synthesis of trans-heterofunctionalized porphyrazine derivatives, J. Organomet. Chem. 63 (1998) 331–336.
[21] W. Szczolko, L. Sobotta, P. Fita, T. Koczorowski, M. Mikus, M. Gdaniec, A. Orzechowska, K. Burda, S. Sobiak, M. Wierzchowski, J. Mielcarek, E. Tykarska, T. Goslinski, Synthesis, characteristics and photochemical studies of novel porphyrazines possessing peripheral 2,5-dimethylpyrrol-1-yl and dimethylamino groups, Tetrahedron Lett. 53 (2012) 2040–2044.
[22] S.L.J. Michel, B.M. Hoffman, S.M. Baum, A.G.M. Barrett, Peripherally Functionalized Porphyrazines: Novel Metallomacrocycles with Broad, Untapped Potential, in: K.D. Karlin (Ed.) Prog. Inorg. Chem., Vol. 50, John Wiley & Sons, Inc. 2001, pp. 473–590.
[23] R. Bonnett, G. Martínez, Photobleaching of sensitisers used in photodynamic therapy, Tetrahedron 57 (2001) 9513–9547.
[24] V. Chauke, A. Ogunsipe, M. Durmuş, T. Nyokong, Novel gallium(III) phthalocyanine derivatives — synthesis, photophysics and photochemistry, Polyhedron 26 (2007) 2663–2671.
[25] I. Seotsanyana-Mokhosi, N. Kuznetsova, T. Nyokong, Photochemical studies of tetra-2, 3-pyridinoporphyrazines, J. Photochem. Photobiol. A Chem. 140 (2001) 215–222.
[26] N.A. Kuznetsova, V.V. Okunchikov, V.M. Derkacheva, O.L. Kaliya, E.A. Lukyanets, Photooxidation of metallophthalocyanines: the effects of singlet oxygen and PcM–O_2 complex formation, J. Porphyrins Phthalocyanines 9 (2005) 393–397.
[27] N.A. Kuznetsova, O.L. Kaliya, Oxidative photobleaching of phthalocyanines in solution, J. Porphyrins Phthalocyanines 16 (2012) 705–712.
[28] K. Ishii, Functional singlet oxygen generators based on phthalocyanines, Coord. Chem. Rev. 256 (2012) 1556–1568.
[29] M.C. DeRosa, R.J. Crutchley, Photosensitized singlet oxygen and its applications, Coord. Chem. Rev. 233 (2002) 351–371.
[30] W. Spiller, H. Kliesch, D. Woehrle, S. Hackbarth, B. Roeder, G. Schnurpfeil, Singlet oxygen quantum yields of different photosensitizers in polar solvents and micellar solutions, J. Porphyrins Phthalocyanines 2 (1998) 145–158.
[31] A. Ogunsipe, D. Maree, T. Nyokong, Solvent effects on the photochemical and fluorescence properties of zinc phthalocyanine derivatives, J. Mol. Struct. 650 (2003) 131–140.
[32] R. Edelson, C. Berger, F. Gasparro, B. Jegasothy, P. Heald, B. Wintroub, E. Vonderheid, R. Knobler, K. Wolff, G. Plewig, Treatment of cutaneous T-cell lymphoma by extracorporeal photochemotherapy, N. Engl. J. Med. 316 (1987) 297–303.
[33] V. Lartillot, A. Risler, Z. Andriamialisoa, M. Giraud, T. Sáe Melo, L. Michel, R. Santus, On the photobiological properties of chimeras combining quaternary ammonium derivatives of retinoic amides and psoralen. A study with cultured human keratinocytes, Photochem. Photobiol. 78 (2003) 623–632.
[34] L. Sobotta, P. Fita, W. Szczolko, M. Wrotynski, M. Wierzchowski, T. Goslinski, J. Mielcarek, Functional singlet oxygen generators based on porphyrazines with peripheral 2,5-dimethylpyrrol-1-yl and dimethylamino groups, J. Photochem. Photobiol. A Chem. 269 (2013) 9–16.